Chapter 13
Surgical Approaches to Medullary Tumors

Helmut Bertalanffy, Souvik Kar, and Christian Hartmann

Abbreviations

cIMPACT-NOW	Consortium to Inform Molecular and Practical Approaches to CNS Tumor Taxonomy
CSF	Cerebrospinal fluid
CT	Computed tomography
DIPG	Diffuse intrinsic pontine glioma
DMG	Diffuse midline glioma WHO grade IV H3 K27M-mutant
GG	Ganglioglioma
GTR	Gross total resection
IDH	Isocitrate dehydrogenase
MAPK	Mitogen-activated protein kinase
MRI	Magnetic resonance imaging
NTR	Near total resection
PA	Pilocytic astrocytoma
PET	Positron emission tomography
PICA	Posterior inferior cerebellar artery
WHO	World Health Organization

H. Bertalanffy (✉)
Vascular Neurosurgery, International Neuroscience Institute, Hannover, Germany
e-mail: bertalanffy@ini-hannover.de

S. Kar
International Neuroscience Institute, Hannover, Germany

C. Hartmann
Department of Neuropathology, Institute of Pathology, Hannover Medical School – MHH, Hannover, Germany

G. I. Jallo et al. (eds.), *Brainstem Tumors*,
https://doi.org/10.1007/978-3-030-38774-7_13

13.1 Introduction

Gliomas of the medulla oblongata (bulbar gliomas) belong to a heterogeneous group of brainstem gliomas. These tumors arise within the medulla and may extend into adjacent structures such as the pons, inferior cerebellar peduncle, cerebellum, and upper spinal cord. Bulbar gliomas occur in children as well as in adult patients. However, their biology differ between pediatric and adult individuals [11]. While brainstem gliomas account for almost one-fifth of all pediatric brain tumors, they account for only less than 2% of all adult gliomas [26]. Among all brainstem gliomas, approximately one-fourth originate within the medulla oblongata [2]. Considered together, medullary gliomas form a heterogeneous group of several tumor entities, rendering it difficult to predict the overall prognosis. Exophytic bulbar gliomas seem to occur more frequently in children and are generally considered more favorable in terms of operability and postsurgical outcomes [22].

This chapter intends to demonstrate that microsurgical resection of medullary gliomas is possible in a well-selected patient population with a low complication rate and a favorable clinical outcome.

13.2 Clinical Presentation

The clinical features of bulbar gliomas reflect their location within the medulla oblongata. Frequent symptoms are lower cranial nerve dysfunction (dysphagia, dysphonia, tongue deviation), cerebellar dysfunction (ataxia, gait disturbance, tremor), and long-tract signs with sensory and motor deficits. Occasionally, tracheostomy and nasogastric tube feeding become necessary in an advanced stage of the disease. Symptoms may develop insidiously and can fluctuate, but they generally tend to deteriorate without appropriate treatment.

13.3 Neuroradiological Evaluation

The primary and most important diagnostic tool is the magnetic resonance imaging (MRI) with various sequences, including T1-weighted contrast-enhanced images. In rare instances, computed tomography (CT) scans may show evidence of intratumoral calcifications. On MRI, the most important morphological aspects of the underlying tumor become evident: focal or diffuse parenchymal infiltration, cystic and exophytic components, size, and degree of extension into adjacent structures. The majority of focal bulbar gliomas are low-grade tumors; they are generally more suitable for surgical resection than diffusely infiltrating tumors, which occur mostly in the pons and less frequently within the medulla.

In addition to MRI, spectroscopy and positron emission tomography (PET) may help in excluding other pathological entities within the medulla such as an abscess,

inflammation, demyelination, vascular malformation, metastatic tumor, ependymoma, or focal ischemia.

13.4 Management Strategies

In contrast to many gliomas located in other parts of the brain, bulbar gliomas and brainstem gliomas are generally not regarded as good candidates for surgical resection. Frequently, the term 'brainstem glioma' is associated with inoperability without further specification. On one hand, this may be understandable since a significant number of brainstem gliomas, particularly in children, are diffuse intrinsic pontine gliomas (DIPGs), which certainly cannot be treated reasonably with surgery. On the other hand, many neurosurgeons are reluctant to attempt extensive microsurgical resection even in focal bulbar (and pontine and mesencephalic) gliomas because of the anticipated postoperative disabling symptoms [11]. Therefore, tumor debulking or only a limited biopsy is preferred in many instances, followed by radio-chemotherapy.

In recent years, however, several reports describing successful surgical resection of brainstem gliomas, including bulbar tumors, were published. Individuals harboring dorsally exophytic or cervicomedullary tumors were carefully selected for surgery, which resulted in better prognosis for patients suffering from such focal gliomas [1, 4, 12, 13, 25, 30]. Surgery was complemented by standard radiotherapy combined with chemotherapy using various agents to achieve a satisfactory long-term result [25].

13.5 Our Patient Series

For more than two decades, the senior author (HB) has focused on brainstem surgery and has microsurgically treated almost 500 patients suffering from various intrinsic brainstem lesions, including gliomas, ependymomas, and cavernous malformations [2]. This large patient series also comprises 43 adult and pediatric patients who harbored a bulbar glioma and underwent microsurgical tumor removal by the senior author in the period of 1996–2019; this group constitutes the patient population discussed in this chapter.

13.5.1 Patient Selection

No precise and widely accepted selection criteria are available in the pertinent literature for bulbar gliomas. Generally, focal, dorsally exophytic and cervicomedullary gliomas have been treated surgically so far; however, the number of published reports on this subject is rather limited [13].

The senior author has applied a differentiated view on every single tumor of this series and selected the patients in a highly individualized fashion based on his previous experience with brainstem surgery and his personal assessment of reasonable operability in each case. A reasonable operability was considered mainly in focal bulbar tumors either confined to the medulla or extending extra-axially in an exophytic manner, in which a significant amount of the lesion (generally, at least half of tumor volume) was expected to be removed without causing additional permanent neurological morbidity. In very few cases, only partial tumor removal (extended biopsy) appeared to be indicated, mainly in order to establish a precise histopathological diagnosis based on the latest tumor classification system. The senior author selected 43 individuals who fulfilled these criteria and treated them microsurgically. Table 13.1 summarizes the characteristics of this subpopulation of brainstem glioma cases.

13.5.2 Tumor Characteristics

This patient series comprises exclusively astrocytic, oligodendroglial, neuronal and mixed-neuronal-glial tumors found in children as well as in adults. Ependymal or other tumor entities affecting the brainstem were not considered here because of their different characteristics and behavior.

Table 13.1 Patient characteristics and tumor entities

Patients	*n* = 43
Females/Males	20/23
Mean age (years)	26.65 (STD ± 18.37)
Median age (years)	27
Age range (years)	1–67
Pediatric group	***n* = 16**
Females/Males	10/6
Mean age (years)	8.37 (STD ± 5)
Median age (years)	7
Age range (years)	1–17
Adult group	***n* = 27**
Females/Males	10/17
Mean age (years)	38.83 (STD ± 12.98)
Median age (years)	35
Age range (years)	21–67
Tumor entities	
Pilocytic astrocytoma	16 (9)[a]
Anaplastic astrocytoma	14 (2)[a]
Ganglioglioma	8 (5)[a]
Glioblastoma	5 (0)[a]

Abbreviations: *n* number, *STD* standard deviation
[a](in parenthesis), number of pediatric cases

13.5.2.1 Tumor Location and Extent

As exemplified in Fig. 13.1, the bulbar gliomas encountered in this patient series varied in their morphological aspect. We distinguished 4 different types, resulting in a sub-classification that appeared helpful in choosing the appropriate surgical exposure; thirteen tumors were confined to the lower brainstem (medullary intrinsic type); other lesions grew exophytically, mainly in lateral (9 tumors) or mainly in posterior direction (13 tumors), while the remaining 8 gliomas extended inferiorly from the medulla into the spinal cord (Table 13.2).

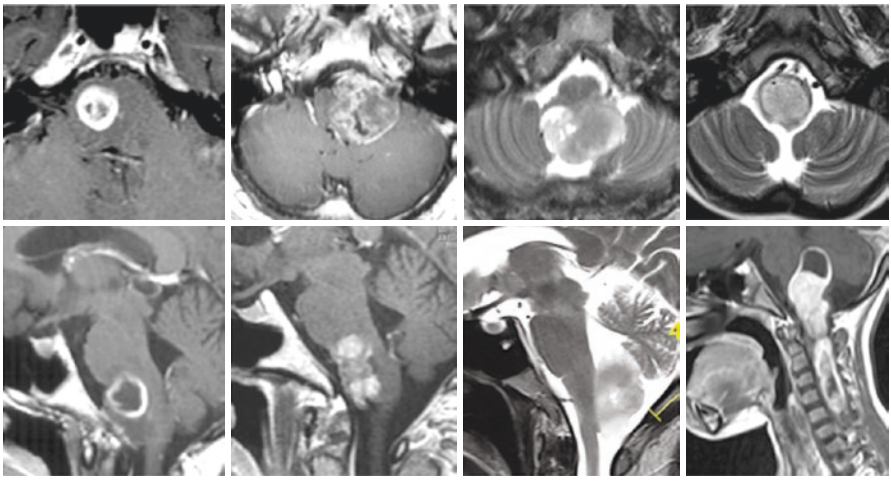

Fig. 13.1 Axial and sagittal MRI scans show representative examples of bulbar tumor location and extent. Each of the 4 columns corresponds to a different patient from this series. Abbreviations: aA anaplastic astrocytoma, f female, *GBM* glioblastoma, m male, PA pilocytic astrocytoma, yrs years

Table 13.2 Tumor location and extent

Pathology/Location and Extent	Intrinsic	Laterally Exophytic	Dorsally Exophytic	Dorsally Exophytic with Cervical Extension	*n*
Pilocytic astrocytoma	5	5	2	4	16
Anaplastic astrocytoma	5	2	4	3	14
Ganglioglioma	0	2	5	1	8
Glioblastoma	3	0	2	0	5
Total	**13** (30.2%)	**9** (21%)	**13** (30.2%)	**8** (18.6%)	**43**

Abbreviation: *n* number

13.5.2.2 Tumor Entities

Four different histopathological tumor entities were encountered in the medulla: pilocytic astrocytoma (PA), anaplastic astrocytoma, ganglioglioma (GG), and glioblastoma (see Table 13.1). While the majority of these lesions emerged as well-circumscribed tumors (see Fig. 13.1), others diffusely infiltrated the lower brainstem and adjacent structures.

Interestingly, no additional tumor entities that we found in the pons or in the midbrain of other patients, such as fibrillary astrocytoma, rosette-forming glioneuronal tumor, anaplastic GG, papillary glioneuronal tumor, pleomorphic xanthoastrocytoma, and anaplastic oligodendroglioma [2], were encountered in this patient series of medullary gliomas.

13.5.2.3 Molecular Signature

Up until the revised fourth edition of the 2016 World Health Organization (WHO) Brain Tumor Classification [19], brainstem gliomas were classified and graded in the same fashion as supratentorial lesions. However, the significant amount of new scientific evidence, particularly those on the molecular signature, mandated an updated classification of these tumors.

High-Grade Brainstem Gliomas

A new entity, the diffuse midline glioma WHO grade IV H3 K27M-mutant (DMG) was introduced into the WHO classification in 2016 [19]. DMG is defined as a glial tumor with an H3 K27M mutation, which occurs in the midline region of the brain, i.e., from the diencephalon to the spinal cord, thus also encompassing the medulla oblongata. Histopathological grading criteria of diffuse (supratentorial) gliomas were regarded as irrelevant for this lesion, so that a WHO grade IV was inevitably assigned to corresponding tumors upon detection of an H3 K27M mutation. In the meantime, however, other tumors have been reported to also emerge in the midline region with histopathological resemblance to ependymomas [8], GGs [16, 17], and PAs [20], as well as exhibiting an H3 K27M mutation. Therefore, in the Consortium to Inform Molecular and Practical Approaches to CNS Tumor Taxonomy (cIMPACT-NOW) Update 3, the DMG definition was complemented by the criterion of diffuse infiltration to avoid the necessity of diagnosing the other entities as WHO grade IV lesions [3]. A systematic analysis regarding the frequency of diffuse gliomas with an H3 K27M mutation in the medulla oblongata is currently not available; consequently, data on this question have to be extrapolated from information on all DMGs. Furthermore, the situation is complicated by the fact that significantly more scientific findings have been published in pediatric than in adult patients regarding the proportion of diffuse gliomas with an H3 K27M mutation, and it remains unclear whether the distribu-

tion pattern remains stable throughout different life decades. Currently, it is assumed that up to 80% of all diffuse gliomas of the brainstem have an H3 K27M mutation and can be classified as DMG [28, 29, 31]. The remaining diffuse gliomas of the brainstem show the molecular signature of supratentorial lesions such as an isocitrate dehydrogenase (IDH) mutation, *EGFR* amplification and/or *CDKN2A* deletions [32]. Interestingly, however, infratentorial gliomas show significantly fewer *IDH1* and *IDH2* mutations than supratentorial gliomas [7, 14, 26], where the R132H variant is found predominantly in about 90% of cases [10]. It is unclear whether, and to what extent, the grading criteria of supratentorial gliomas also have infratentorial validity in the absence of an H3 K27M mutation. However, according to the current WHO classification, only a histopathological grading (diffuse astrocytoma WHO grade II, anaplastic astrocytoma WHO grade III, glioblastoma WHO grade IV) of infratentorial diffuse gliomas with a negative H3 K27M status is recommended [19].

Fourteen patients of the present series were diagnosed as harboring an anaplastic astrocytoma of the medulla (Fig. 13.2), while 5 other individuals suffered from a bulbar glioblastoma. The MRI scans of 1 glioblastoma patient are shown in Fig. 13.1 (*leftmost column*), while those of 3 other patients can be seen in Fig. 13.3.

Pilocytic Astrocytoma

PAs are tumors that usually exhibit a clearly demarcated border to the adjacent brain parenchyma; they continue to be assigned to a WHO grade I by the WHO classification [19]. Extensive molecular analyses have shown that all PAs usually have a mutation in 1 gene of the mitogen-activated protein kinase (MAPK) pathway, indicating that these lesions are single pathway tumors [15]. While cerebellar PAs show *BRAF*:*KIAA1549* duplication and fusion in almost all cases, a corresponding genetic alteration is found in only about 60% of extracerebellar tumors of this type. Extracerebellar PA alternately shows *BRAF* V600E, *FGFR1*, *NF1* and *NTRK2* mutations [15]. The molecular profile of PA of the medulla has not been systematically investigated yet. It is assumed that bulbar PAs show genetic alterations comparable to all other extracerebellar tumors of this type. While the current WHO classification only discusses the possibility of anaplastic PA [19], a corresponding entity could perhaps be defined molecularly. The most common single genetic change in these anaplastic PAs is the homozygous *CDKN2A* deletion [24].

Presently, brainstem gliomas with typical histopathological characteristics of PAs, as well as those with diffuse parenchymal infiltration and concomitant H3 K27M mutation, constitute an unsolved problem. Several publications imply that patients harboring such tumors have a significantly worse prognosis. Indeed, we also could observe an unexpectedly unfavorable clinical course in 2 patients of this series who harbored a bulbar glioma that was histopathologically classified as

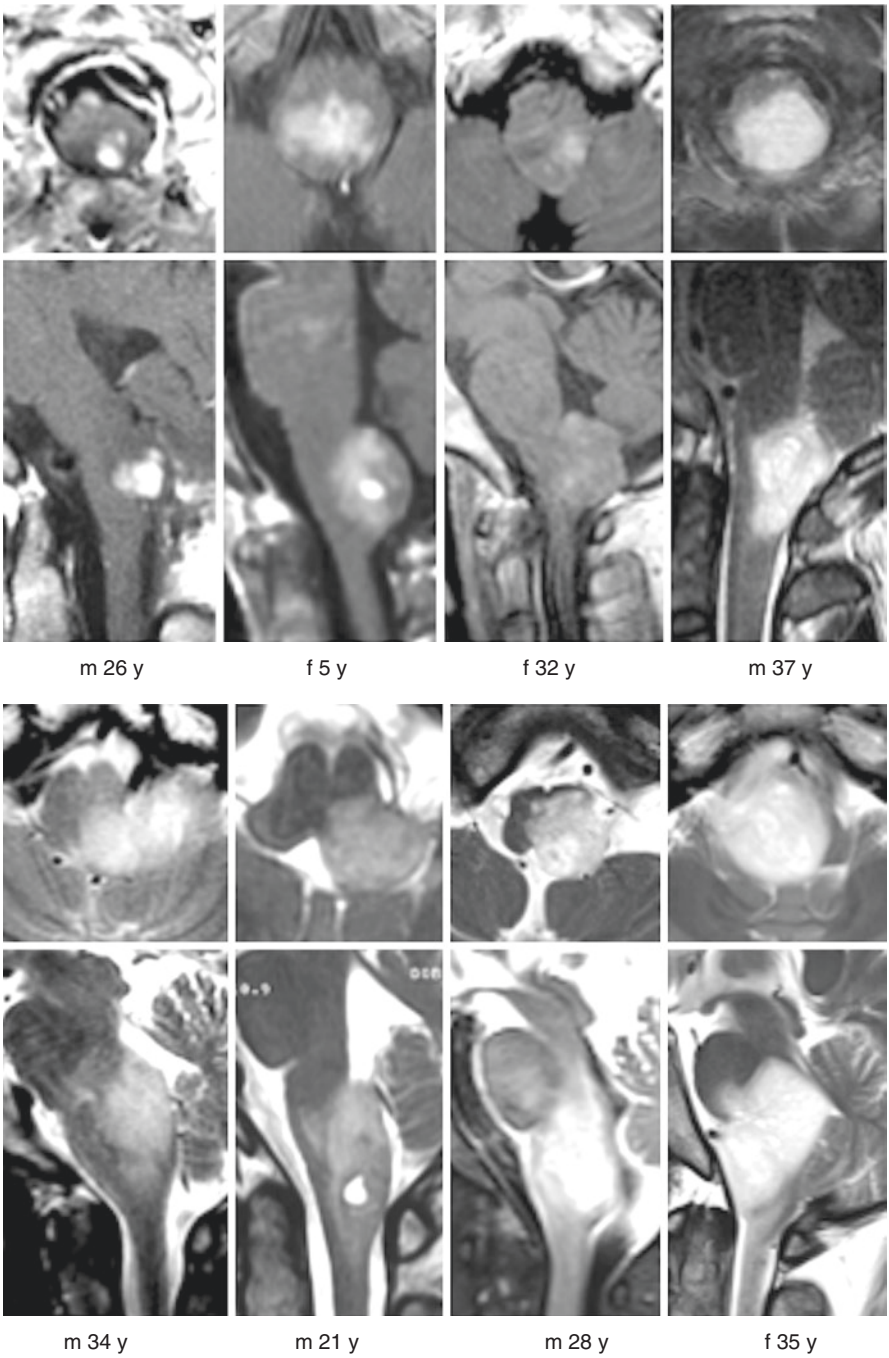

Fig. 13.2 Axial and sagittal MRI scans show typical anaplastic astrocytomas arising from the medulla oblongata. Each column with axial and sagittal MRI, respectively, corresponds to one of 8 illustrative cases from the present surgical series. Abbreviations: f female, m male, y years

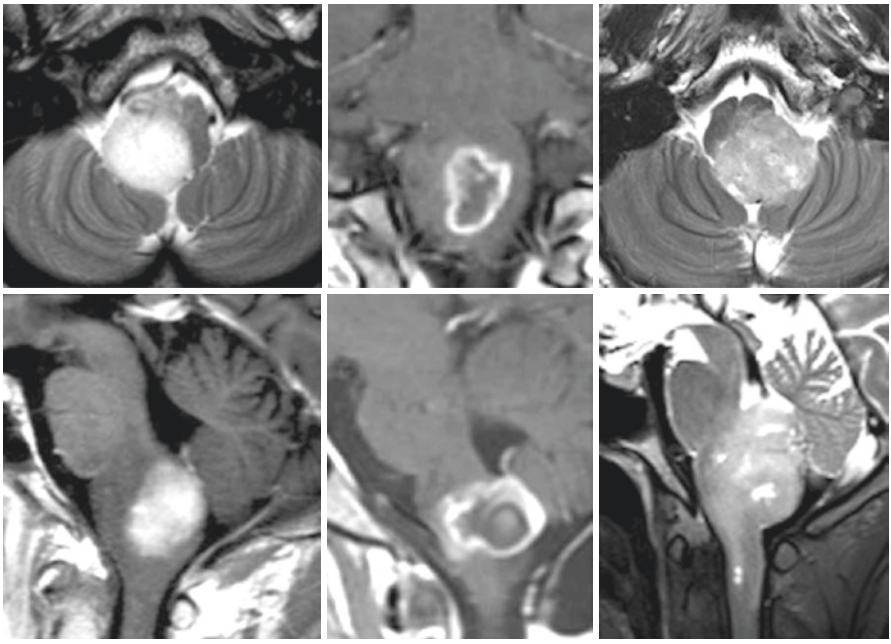

Fig. 13.3 Axial and sagittal MRI scans of 3 patients from this series who harbored a glioblastoma. Abbreviations: m male, yrs years

PA. One of them is exemplified in Figs. 13.4 and 13.5. In this context, some authors have characterized such tumors as anaplastic PAs [6, 23]. However, it appears worthwhile to attempt clarifying in the future whether a tumor with morphological features of a PA and concomitant H3 K27M mutation actually corresponds to a DMG WHO grade IV when epigenetic analyses, early tumor recurrence, and patient's overall reduced survival are taken into account.

The present patient series comprises 16 individuals who harbored a bulbar PA (Fig. 13.6).

Ganglioglioma

GG WHO grade I, and the very rare anaplastic GG WHO grade III, typically show a *BRAF* V600E mutation [19]. However, the reported mutation frequency of *BRAF* V600E varies between 20% and 60% [18, 27]. The histopathological architecture of GG is thought to explain these significant differences: the tumors show much smaller ganglion cell and glial components. If the *BRAF* V600E status is determined using a mutation-specific antibody rather than genetically, it can sometimes be demonstrated that only the ganglion cell component expresses the mutated protein. It is assumed that the number of tumor DNA with a *BRAF* V600E mutation is partially below the detection limit. Consequently, these tumors are then identified as *BRAF* wild-type in the genetic analysis, although

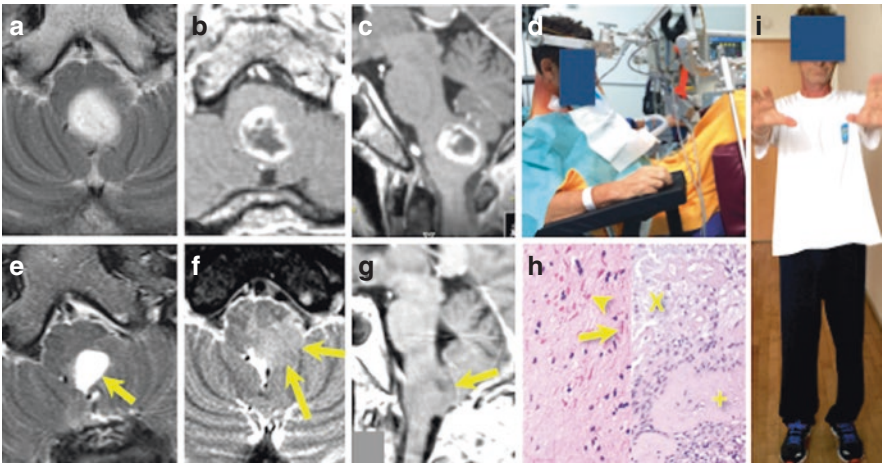

Fig. 13.4 Ten months prior to surgery, this 56-year-old man developed progressive dysphagia, imbalance, slight right-sided hemiparesis, and left-sided hemihyperesthesia. Preoperative T2-weighted axial (**a**) and contrast-enhanced T1-weighted axial and sagittal MRI (**b**, **c**) show evidence of an intrinsic tumor of the medulla. The patient underwent surgery in the semi-sitting position (**d**) via midline suboccipital craniotomy, including the posterior rim of the foramen magnum and combined with C1 laminectomy. Postoperative MRI documented gross total tumor resection (**e**, arrow). Only 3 months later, however, the patient developed new symptoms, and a local tumor recurrence was detected on a follow-up MRI (**f** and **g**, arrows). Histopathological examination (**h**) showed a predominantly biphasic, astrocytic tumor with low cellularity, which contained Rosenthal fibers (arrow), protein droplets (arrowhead), and, in various locations, hyalinized blood vessels (+) and small areas of necrosis (X). The final diagnosis was pilocytic astrocytoma (PA) WHO grade I without any signs of anaplasia. As the patient did very well immediately after the surgical intervention, and since there were no additional neurological deficits by that time (**i**), the diagnosis of PA was not questioned initially. Following the early local tumor recurrence, however, we suspected the presence of a diffuse midline glioma (DMG) despite the former histopathological diagnosis. Subsequently, the patient underwent combined radio-chemotherapy

the small ganglion cell component actually has the mutation [18]. The processing of the *BRAF* wild-type GG revealed that these tumors, similar to PAs, also show mutations in genes of the MAPK pathway [21]. GGs of the posterior fossa and spinal cord, as well as bulbar GGs with *BRAF* V600E mutations, were divided into two groups: (a) classical GGs with *BRAF* V600E mutation and (b) PAs with gangliocytoma differentiation, which typically exhibited *BRAF*:*KIAA1549* duplication and fusion [9]. In summary, it can be concluded that there are frequent morphological overlaps in the group of glial/glioneuronal tumors [19], and that these tumors are also epigenetically related to each other [5].

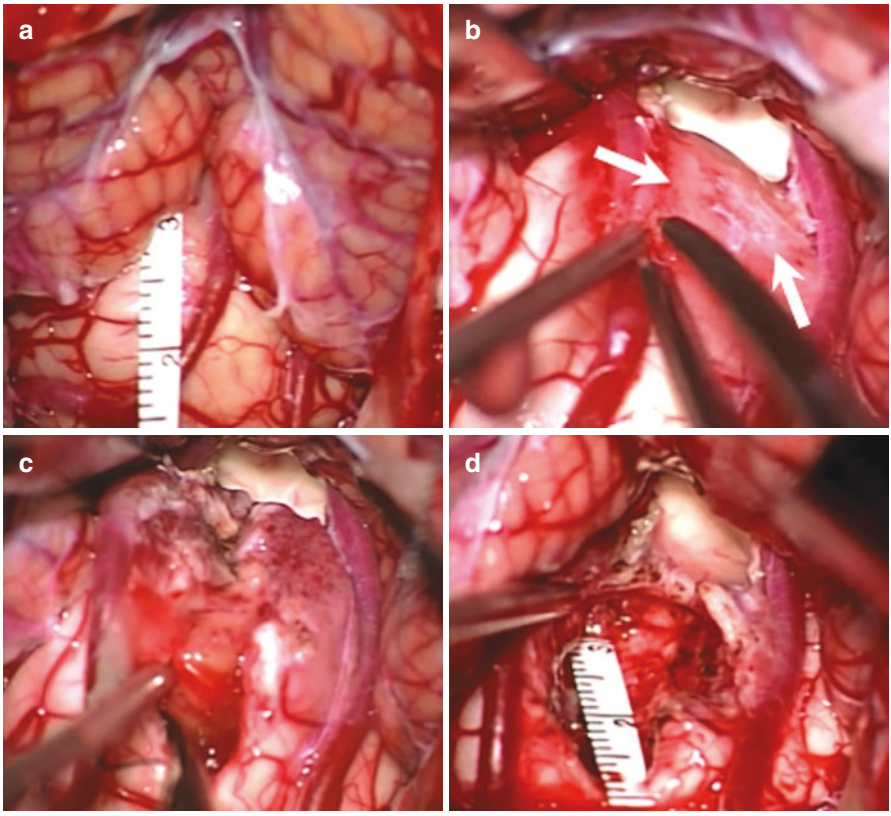

Fig. 13.5 Intraoperative photographs of the patient shown in Fig. 13.4. After opening the dura mater, the surface of the medulla appeared bulging posteriorly between the cerebellar tonsils due to the underlying tumor. A millimeter scale demonstrates the local dimensions (**a**). Adhesions (arrows) between the reddish tumor surface and cerebellum were present. After detaching the tumorous medulla from the cerebellum, the rhomboid fossa became visible above the lesion (**b**). Enough tumor tissue was harvested for histopathological examination (revealing a pilocytic astrocytoma), and the tumor was gradually diminished in volume with the aid of an ultrasonic aspirator. Obviously, there was no clear dissection plane between lesion and brainstem parenchyma (**c**). Eventually, gross total tumor resection was achieved as could be estimated macroscopically. The millimeter scale placed into the tumor resection cavity helped in determining the extent of safe tumor removal (**d**)

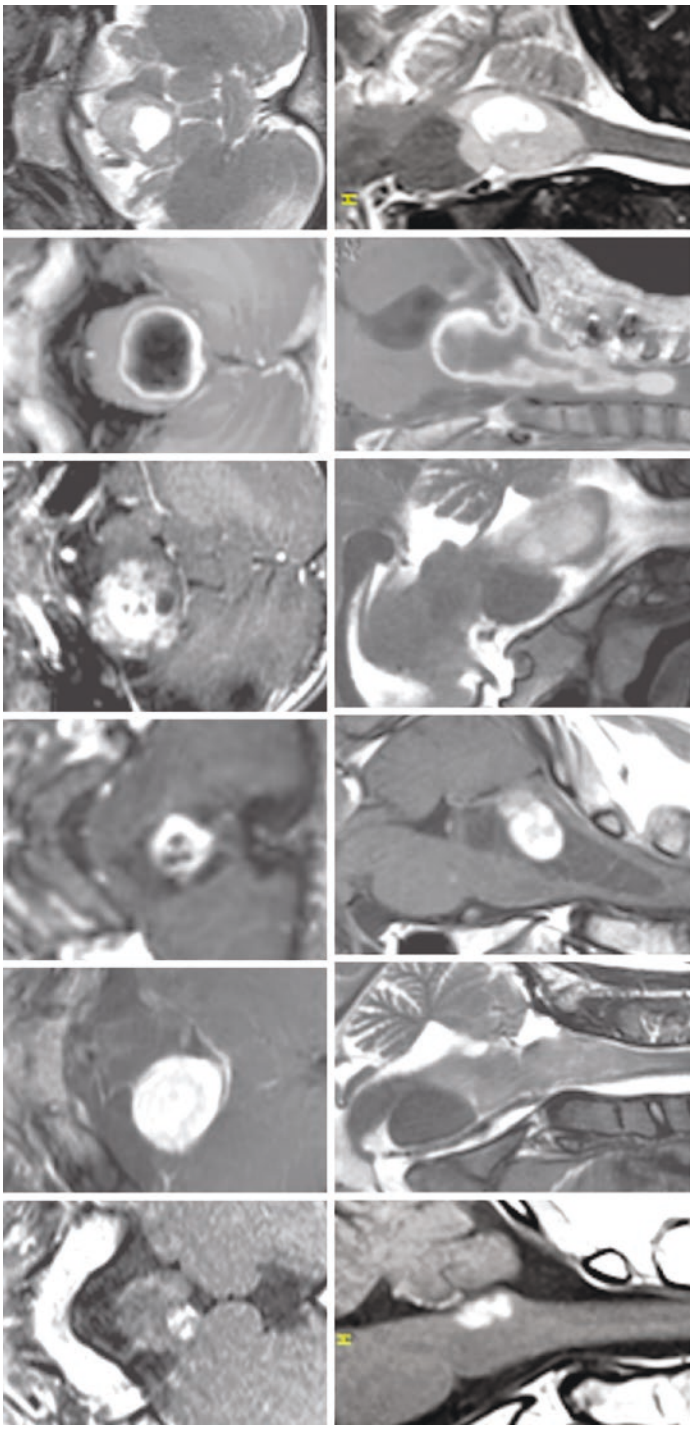

Fig. 13.6 Axial and sagittal MRI scans show typical pilocytic astrocytomas of the medulla oblongata. The images belong to 6 illustrative cases from the present surgical series, with each column representing a different individual. Patients shown here were aged 4–61 years. Abbreviations: f female, m male, yrs years

In the present series we have selected 8 individuals harboring a bulbar GG for microsurgical treatment (Fig. 13.7).

13.5.3 Surgical Strategies

Surgery, the mainstay of therapy for low-grade gliomas in other intracranial locations, was also considered in low-grade gliomas of the medulla. The role of surgery in high-grade bulbar gliomas has not yet been established. Despite the poor prognosis, we have attempted surgery in these malignant tumors as well, hoping to achieve a comprehensible benefit for the patient in these cases.

Once the indication for surgery has been established in a patient, we proceed with defining the goals of surgery and precisely planning the procedure.

13.5.3.1 Goals of Surgery

In principle, the surgery is aimed primarily at removing as much of the pathological tissue as possible without damaging the underlying central nervous system paren-

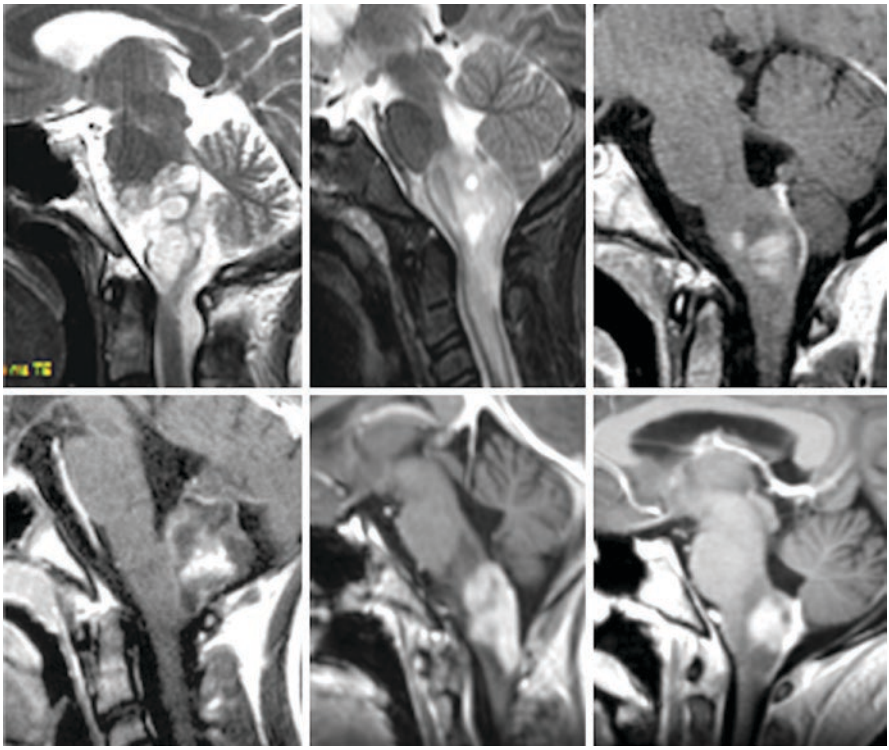

Fig. 13.7 Sagittal MRI scans demonstrate typical bulbar gangliogliomas. Each image belongs to one of 6 illustrative cases from the present surgical series. The patients were aged 8–53 years

chyma. The main goal was to decompress the brainstem and interrupt the pathological mechanism of long tracts and bulbar nuclei damage caused by the tumor. In high-grade gliomas, we attempted to achieve at least a better result than just good palliative care in terms of prolonging the patient's survival with an acceptable quality of life. In well-circumscribed lesions, we attempted to achieve a total or near-total tumor removal, while tumor volume reduction without an attempt of radical resection appeared as a reasonable alternative in less well-delineated low-grade tumors, or in high-grade tumors that usually lacked a clear demarcation toward the brainstem or spinal cord parenchyma. Deliberate partial tumor volume reduction was the goal in rather very voluminous symptomatic tumors, in which radical resection would have been possible only at the price of significant clinical deterioration.

13.5.3.2 Timing of Surgery

In patients in whom a bulbar glioma was suspected and the lesion appeared operable, we recommended surgery in the near future to avoid further tumor progression and possible clinical deterioration. Rapidly progressing symptoms, however, required surgery without further delay. Observation and repeat MRI were generally indicated only in individuals presenting with mild symptoms and in a stable clinical condition, in whom the diagnosis remained unclear after an initial MRI examination.

13.5.3.3 Preoperative Planning and Tumor Exposure

In each case, we tailored the surgical approach according to the morphological features of the underlying bulbar glioma. For preoperative planning, we used a high-quality MRI, and in cervicomedullary tumors, we also utilized CT scans of the upper cervical spine with a bone window technique to assess the exact shape of the vertebrae. We informed the patients and their families about the goals of surgery in detail, the specific possibilities of tumor resection, and the risks associated with the planned procedure. To be prepared for adequate therapeutic measures, we preoperatively discussed with our anesthetists the possible occurrence of intraoperative vagal reaction with sudden bradycardia or a sudden rise in blood pressure due to manipulation within the medulla oblongata.

While intraoperative neuronavigation played almost no role in the surgery of bulbar gliomas, continuous electrophysiological monitoring was a mandatory tool that was applied in all surgical procedures. Somatosensory and motor evoked potentials were routinely used throughout the intervention. In some instances, we also used intraoperative electromyography of the vagal and hypoglossal nuclei.

Surgical access to the medulla was usually less demanding than exposing the pons or the midbrain. Basically, we used only two access routes to resect tumors confined to the medulla: a standard midline suboccipital exposure with opening of the foramen magnum posteriorly (*see* Sect. 12.6.1 of Chap. 12 for detailed description of the medial suboccipital approach and surgical technique), and a lateral suboccipital exposure that was sometimes extended laterally and inferiorly (paracondylar

or transcondylar exposure) for laterally exophytic tumors (see the section below for detailed description of the far-lateral approach and surgical technique). We always expose the floor of the fourth ventricle (rhomboid fossa) by dissecting between the cerebellar tonsils and uvula, and by transecting the posterior medullary velum and tela choroidea (telovelar exposure). In a few instances, particularly for dorsally exophytic tumors with significant lateral extension, we applied a combined lateral and midline exposure that was necessary to sufficiently expose the entire lesion (Fig. 13.8).

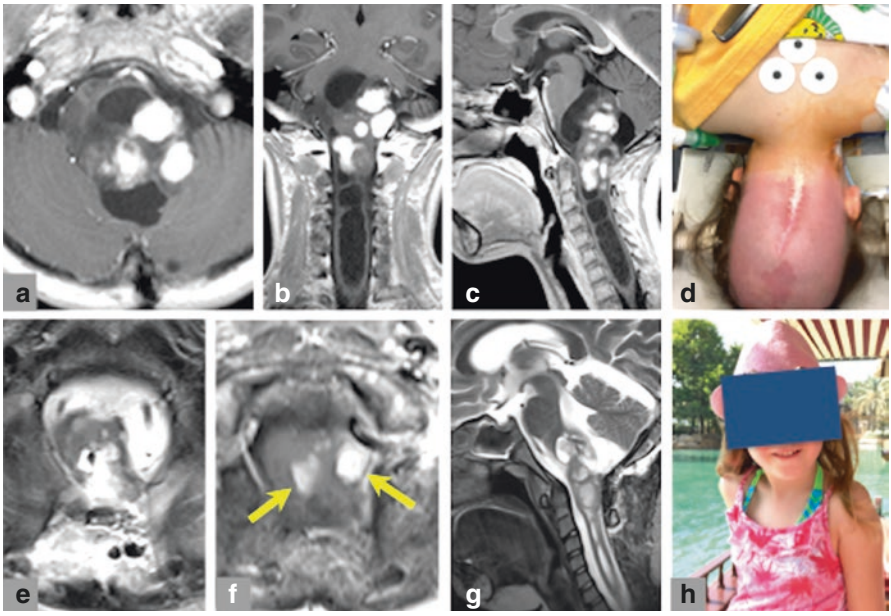

Fig. 13.8 This 8-year-old girl became symptomatic at the age of 1.5 years when her parents observed a slight limping in her left leg. Years later, following detection of a large craniocervical tumor, the girl underwent suboccipital craniotomy at another institution. By that time, the surgical procedure consisted of local tumor biopsy and enlargement of the dura mater (duraplasty). Histopathological examination revealed the presence of a pilocytic astrocytoma, and chemotherapy with Vincristine and steroid medications were initiated. Subsequently, however, there was no detectable change of the lesion size on MRI. The tumor originated from the posterior medulla and consisted of large contrast-enhancing portions in addition to non-enhancing areas combined with adjacent cysts. The tumor mass had invaded the upper cervical cord reaching the C3 level and caused a space-occupying intramedullary syrinx extending inferiorly to the T1 level (**a**–**c**). Clinically, slight left-sided hemiparesis was noted. Tumor volume reduction became necessary at this stage because of repeated matutinal nausea and vomiting despite steroid medications. Surgery was undertaken with the child in the prone position and the head placed in the headrest coil unit for intraoperative MRI scanning (**d**). Tumor exposure was carried out again via a suboccipital craniotomy and an additional C1 laminectomy and C2 and C3 laminoplasty. Postoperative MRIs documented a significant tumor volume reduction of approximately 80–90% and small contrast-enhancing residual tumor portions (**e**–**g**, arrows). There were no perioperative complications, and no additional neurological deficits occurred. The child tolerated the surgical intervention without problems and was mobilized from the second postoperative day. Two years after surgery (**h**), the girl is neurologically intact with stable tumor remnants on control MRI

Although not described in this series, tumors confined to the pontomedullary junction and upper medulla or exophyting into the cerebellomedullary cistern can be tackled with a retrosigmoid approach (see Sect. 12.5.2 of Chap. 12 for detailed description of the retrosigmoid approach and surgical technique). Cervicomedullary tumors always required an additional exposure of the upper spinal cord, achieved by C1 laminectomy and C2 laminotomy down to the caudal tumor extension (Fig. 13.8), sometimes down to the level of C7 or T1 in very extensive lesions. At the end of the intradural procedure, we usually replaced the blocks of spinous processes and vertebral laminae and fixed them *in situ* with osteosynthetic titanium microplates and screws (cervical laminoplasty).

Far-Lateral Approach

The far-lateral approach permits access to the cisterna magna, cerebellomedullary and premedullary cisterns, exposing the antero-lateral and posterior surfaces of the medulla oblongata. Compared to a suboccipital craniotomy that only exposes the posterior surface of the medulla, the far-lateral approach is most suitable to resect medullary tumors through the antero-lateral safe entry zones, namely the pre-olivary sulcus (limited by the pyramidal tract anteriorly and the olive posteriorly) and the retro-olivary sulcus (limited by the olive anteriorly and the inferior cerebellar peduncle and cranial nerves IX/X posteriorly). The transcondylar, supracondylar and paracondylar variants of the far-lateral approach are extensions of a basic lateral suboccipital craniotomy. Although the paracondylar variant is mostly used to expose lesions involving the lateral aspect of the clivus and jugular process as opposed to the transcondylar and supracondylar variants that provide access to the antero-lateral surface of the medulla oblongata, all three variants are described below for the sake of completion. The far-lateral approach maybe combined with transmastoid and/or supratentorial approaches to access higher levels of lateral and antero-lateral aspects of the brainstem.

The patient is usually positioned in the three-quarter prone (a.k.a. park bench) position, where the patient side that is ipsilateral to the lesion is elevated at 45° from a prone position, and the head is rotated 45° to the contralateral side of the lesion with lateral flexion to the floor. The skin can be incised in two ways: the lazy S incision is relatively smaller than the inverted hockey stick incision, starting around the Asterion level, passing through the foramen magnum level, and ending with a medial curvature towards the C2 spinous process; whereas the inverted hockey stick incision follows a much longer trajectory, starting at 2 cm below the mastoid tip, proceeds vertically above the level of the superior nuchal line, turns medially towards the inion, then turns again to proceed inferiorly to the C2/C3 level. The wide exposure of the inverted hockey stick incision allows for utilizing the benefits of exposing the C1 transverse process during the paracondylar variant of the far-lateral approach, while the lazy S generally provides exposure for the transcondylar and supracondylar variants only.

The dissection starts by cutting the nuchal muscles (sternocleidomastoid, trapezius, longissimus capitis, splenius capitis, and semispinalis capitis) in a single bundle just below the superior nuchal line, which exposes the suboccipital triangle

(formed by the superior oblique, inferior oblique and rectus capitis posterior major muscles). Within the suboccipital triangle, the vertebral artery (third segment), posterior arch of atlas, and C1 nerve dorsal ramus are then identified after meticulous dissection of the vertebral venous plexus. Care should be taken not injure a posterior inferior cerebellar artery or posterior spinal artery of extradural origin in this region. After reflecting the muscles of the suboccipital triangle, three additional muscles are exposed: rectus capitis posterior minor (medial to the rectus capitis major muscle), rectus capitis lateralis (connects the transverse process of atlas to the inferior surface of the jugular process, just lateral to the occipital condyle; an important landmark for the paracondylar variant of the far-lateral approach), and levator scapulae (originates at the postero-inferior border of the transverse process of the atlas; extends lateral to the second segment of the vertebral artery and medial to the carotid compartment).

Bone window opening proceeds with a lateral suboccipital craniotomy. Important landmarks include the Asterion (just posterior to the sigmoid and inferior to the transverse sinuses), superior nuchal line (approximates the level of the transverse sinus and torcula), and the external occipital crest (medial limit of craniotomy). Part or all of the condylar fossa may be included in the initial craniotomy, where the posterior condylar emissary vein is identified and cauterized. The C2 spinal nerve root courses medial to the atlantoaxial joint and should be protected before the next step. The vertebral artery is then dissected away from the posterior arch of the atlas, the ipsilateral half of which is cut (medially in the midline and laterally close to the lateral mass of atlas) and elevated in one piece after unroofing the foramen transversarium and freeing the vertebral artery; the vertebral artery should now be easily displaced laterally and away from the subsequent craniectomy and dissection field.

The transcondylar variant follows a trajectory to the mid-to-lower antero-lateral medulla and lower clivus and exposes the intracranial segment of the vertebral artery. It starts with drilling the posterior third of the condyle until the posterior wall of the hypoglossal canal (dark blue color due to presence of venous plexus; cortical bone as opposed to the cancellous bone of the condyle) is encountered, then proceeds medial and inferior to the hypoglossal canal to reach the anterior medullary region and clivus.

The supracondylar variant provides access to the upper antero-lateral medulla and foramen magnum, as well as the petroclival junction and mid-clivus. Using a diamond bur, the posterior portion of the jugular tubercle is drilled above the hypoglossal canal and below the sigmoid sinus sitting in the sigmoid compartment of the jugular foramen; the lateral limit is the jugular bulb. Knowing that the glossopharyngeal, vagus and accessory nerves run in the neural compartment (which lies between the sigmoid compartment posteriorly and petrous compartment anteriorly of the jugular foramen), these nerves are exposed medially and are at risk of injury, especially the spinal rootlets of the accessory nerve running along the dura in this area.

The paracondylar has the most lateral trajectory of the three variants and is utilized for lesions involving the jugular process and posterior aspect of the mastoid. Intraoperative neurophysiologic monitoring of cranial nerves IX, X and XI is man-

datory throughout the procedure. It requires raising the posterior belly of the digastric muscle to expose the digastric groove, which will help to locate the exit of the facial nerve through the stylomastoid foramen. Fine drilling using a diamond bur proceeds supero-lateral to the condyle, around the exocranial aspect of the jugular foramen, and is directed towards the jugular process, onto which the rectus capitis lateralis is inserted posterior to the jugular foramen. Optimally, the neural compartment of the jugular foramen, lower and distal sigmoid sinus, jugular bulb, internal jugular vein, and internal carotid artery (pharyngeal segment) are seen in the final exposure.

A wide dural flap is incised, and cerebrospinal fluid (CSF) is drained by opening the cisterna magna; the posterior spinal artery should be identified and protected from this step onwards. The vertebral artery pierces the dura at the infero-medial corner of the occipital condyle, after which it is attached to the atlanto-occipital junction by the intracranial denticulate (dentate) ligament. Along its anteromedial trajectory to join the contralateral vertebral artery, the posterior inferior cerebellar artery (PICA) branches off in the premedullary cistern before the vertebrobasilar junction. Access to the antero-medial compartment of the posterior fossa is granted through the vagoaccessory triangle, bordered by the medulla medially, the vagus and medullary rootlets superiorly, and the body of the accessory nerve laterally. This triangle is also divided into a superior window and an inferior window by the hypoglossal nerve, the latter of which is maximally exposed during the trancondylar variant. The accessory nerve runs posterior to the denate ligament at the spinal level but crosses the ligament as it runs antero-superiorly to exit through the neural compartment of the jugular foramen. The vertebral artery, however, remains anterior to the accessory nerve, thus facilitating dissection towards the lateral medullary surface. By combining the transcondylar and supracondylar variants, angulating the microscope towards the brainstem (as opposed to the petrous bone) allows for maximal access to the upper and lower antero-lateral medullary surface as well as the neurovascular structures in the cerebellomedullary and premedullary cisterns. Visualizing the antero-medial medullary surface, however, is facilitated by the help of angled endoscopes passed through the vagoaccessory triangle.

13.5.3.4 Microsurgical Dissection Technique

We have encountered both gliomas that were easily discernable from the normal brain parenchyma as well as tumors that tended to diffusely infiltrate the brainstem and lacked a plane of dissection, some of which were PAs. In contrast to other tumor entities, GGs showed a tendency toward firm adhesion to adjacent cranial nerve rootlets or blood vessels, thus usually preventing a 100% tumor removal. Generally, many tumors encountered in this series were well-vascularized, gray-reddish in color, soft, and easily aspirated using the suction tube or the ultrasonic aspirator (Fig. 13.9).

With few exceptions, most of the PAs were well-demarcated, and the surrounding brainstem parenchyma was not edematous. GGs were of higher consistency than PAs and appeared as a rather compact tumor tissue. In high-grade gliomas,

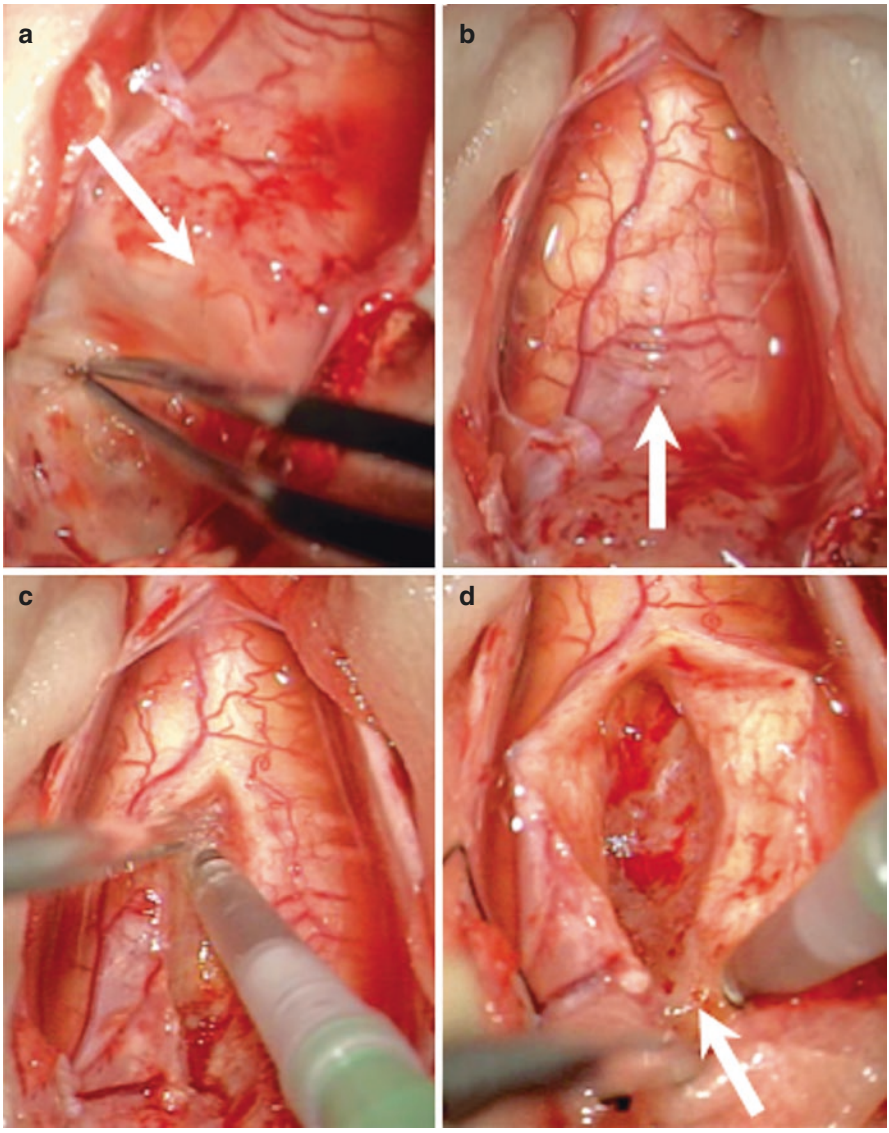

Fig. 13.9 Intraoperative photograph of the patient shown in Fig. 13.8. Due to the initial surgical intervention with tumor biopsy and duraplasty performed at another hospital, severe scar formation and adhesions between the dorsal tumor surface and surrounding structures were encountered, particularly at the level of the transition between the medulla and spinal cord (**a**, arrow). In this area, the tumor had invaded the upper cervical cord in an infiltrative manner (**b**, arrow). Tumor resection was started in the cervical area and was carried out via a midline myelotomy at C1 and C2 levels using the ultrasonic aspirator (**c**). Particularly on the left side, the tumor had diffusely invaded the spinal cord and medulla (**d**, arrow). Consequently, no clearly demarcated dissection plane could be found in this area between the tumor and CNS parenchyma. For safety reasons, small residual tumor portions were therefore deliberately left behind

only rarely did we find a well-defined tumor border. These tumors usually grew in a diffusely infiltrative manner, and the adjacent parenchyma was edematous and contained fragile blood vessels, sometimes rendering local hemostasis quite difficult.

Initially, we started with microsurgical tumor volume reduction in a safe remote region and then gradually worked toward the tumor-parenchyma transition area.

In the 13 intrinsic gliomas of this series, the tumors were not readily visible on the surface of the brainstem. In these cases, we had to choose an optimal entry zone into the medulla. Depending on tumor location, this was either the posterior midline of the medulla (posterior median sulcus, above and/or below the obex) and, in many instances, combined with a midline myelotomy of the upper spinal cord, or the lateral or even anterolateral aspect of the medulla, such as the pre-olivary and retro-olivary sulci. Alternate safe entry zones through the dorsal surface of the medulla also include the posterior intermediate and posterior lateral sulci. Occasionally, during microsurgical tumor dissection within the medulla, sudden bradycardia and/or a significant rise in blood pressure occurred. In such instances, microsurgical manipulation was immediately interrupted for several minutes to allow for the cardiovascular situation to normalize again.

13.5.3.5 Extent of Tumor Resection

In principle, we always attempted removing as much of the tumor mass as deemed safely possible. Not surprisingly, the medulla did not tolerate excessive surgical manipulation because long-tract pathways and cranial nerve nuclei are concentrated here in a tight fashion. In the case of focal tumors in which the pathological tissue was clearly distinguishable from the medullary parenchyma, we were able to remove a larger amount of the tumor without affecting the brainstem parenchyma. Somewhat differently, we resected diffusely infiltrating bulbar tumors only to a certain degree, while correlating the tumor size known from preoperative MRIs with local measurements using a millimeter scale (see Fig. 13.5), and guided by the stability of intraoperative evoked potentials, heart rate, and blood pressure. In every case, we also concentrated on distinguishing tumor feeders from perforating pial arteries supplying the medulla to avoid local ischemic damage.

Table 13.3 gives an overview of the extent of tumor resection according to the underlying tumor entity. In half of our cases (approximately 51%), we achieved

Table 13.3 Extent of tumor resection

Tumor Entity/Extent of Resection	GTR	NTR	STR	Biopsy or Debulking
Pilocytic astrocytoma	8	3	4	1
Anaplastic astrocytoma	3	3	6	2
Ganglioglioma	1	3	3	1
Glioblastoma	0	1	2	2
Total	**12** (27.9%)	**10** (23.2%)	**15** (34.9%)	**6** (14%)

Abbreviations: *GTR* gross-total resection (99–100% of tumor volume removed), *NTR* near-total resection (90–98%), *STR* subtotal resection (50–89%), Biopsy/debulking, (<50%)

Table 13.4 Outcome and surgical characteristics

	Pilocytic Astrocytoma	Anaplastic Astrocytoma	Ganglio-glioma	Glioblastoma
Lost to follow-up	1	3	1	0
No new neurologic deficits	12	11	6	1
Additional morbidity	4	3	2	4
Surgical complications	1	0	0	0
Postoperative tracheostomy required	2	1	0	2
Tumor progression/ recurrence	4	5	2	5
Repeat tumor surgery	2	0	1	1
Disease-related death	2	3	0	5

gross-total resection (GTR) or near-total resection (NTR), which is a quite satisfactory rate for bulbar gliomas. Expectedly, the resection rate was somewhat higher in PAs, even in patients suffering from large tumors. Tumor volume reduction of less than 50% (tumor debulking) was carried out in only 14% of cases, as expected in high-grade tumors.

13.5.4 Clinical Outcome

Fortunately, there was no direct surgical mortality, and no patient suffered from permanently or severely disabling neurological deficits attributable to the surgical intervention. All patients who did not ultimately survive died later on from their primary disease, the bulbar glioma.

Remarkably, no additional neurological deficits occurred in 30 of 43 individuals (approximately 70%) as shown in Table 13.4. Moreover, there was no patient of this series in whom, retrospectively, management of the bulbar glioma would have appeared more favorable without surgical intervention, which also supports our method of patient selection.

13.5.4.1 Pilocytic Astrocytoma

In 12 of 16 individuals suffering from a PA, there were no additional neurological deficits after surgery. Four patients experienced temporary neurological deterioration such as the patient shown in Fig. 13.10, who was the only individual suffering from a postoperative complication, namely CSF leak that required re-operation. Two male patients (56 and 61 years old) passed away due to progression of the tumor at 3 years and 8 months after surgery, respectively. They had experienced no or only mild additional symptoms immediately after surgery, but an early local tumor recurrence occurred in both; one of them is shown in Fig. 13.4. We suspect

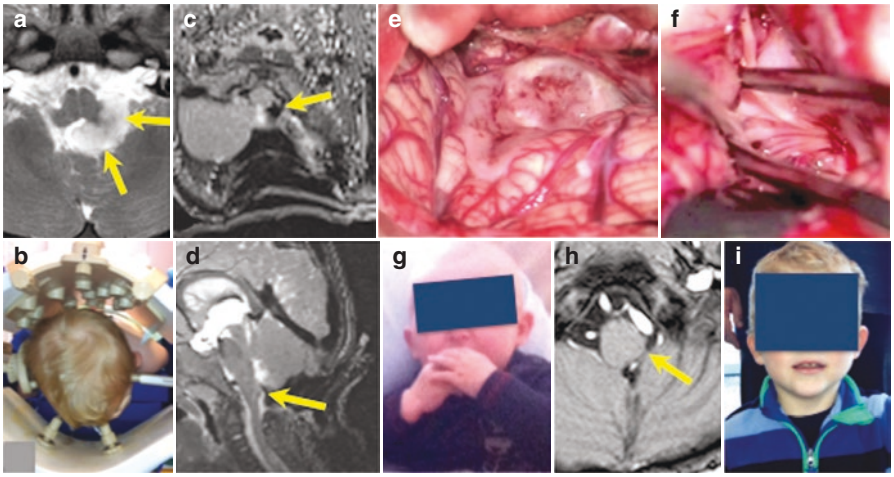

Fig. 13.10 The parents of this 15-month-old boy noticed an abnormal head tilt to the left side in their child since he was 10 months old. Obviously, these symptoms were caused by left-sided partial sixth nerve palsy. Moreover, the child developed recurrent laryngitis. Preoperative MRI revealed a homogeneous tumor originating from the left lateral medulla, which extended posteriorly and laterally (**a**, arrows). The boy underwent surgery in the prone position with the head fixed in a special headrest coil unit (**b**) for intraoperative magnetic resonance imaging (BrainLAB, 1.5-T MR imager Magnetom Espree, Siemens). Intraoperative T1- and T2-weighted images were obtained during surgery to rule out any tumor remnants (**c** and **d**, arrows). The tumor (a pilocytic astrocytoma) was exposed via combined posterior median and left lateral suboccipital craniotomy with wide opening of the foramen magnum. The tumor tissue was homogeneous, of soft consistency, and well distinguishable from the normal brainstem parenchyma (**e**). Tumor volume reduction was carried out with an ultrasonic aspirator. In the left lateral recess, the tumor was adherent to the rootlets of the caudal cranial nerves; nevertheless, it was successfully separated from these structures while preserving their integrity. Gross-total tumor removal was achieved (**f**). Postoperatively, dysphagia precluded oral nutrition for 9–10 days; due to subcutaneous collection of cerebrospinal fluid, the boy underwent a second surgical intervention after 4 days for dural repair. Subsequently, the child's deglutition gradually normalized again, and the boy was symptom-free at 2 weeks after surgery (**g**). Three years after surgery, T1-weighted contrast-enhanced MRIs documented complete tumor removal (**h**), and the boy is in excellent clinical condition without neurological deficits (**i**)

that the diagnosis of PA might not have been accurate in either case. Circumstantial evidence suggests that these individuals may rather have suffered from an anaplastic PA or DMG. Tumor progression was documented in two additional patients during the long-term follow-up, while repeat surgery was carried out in only two of the four individuals at 2 years and 3 years after the first intervention.

13.5.4.2 Ganglioglioma

There were no surgical complications in this subgroup of patients. Only two females, 17 and 53 years old, suffered from postoperative augmentation of preoperative symptoms (facial palsy in one and ataxia in the other), but these symptoms gradually faded away thereafter. Due to local tumor recurrence, one 10-year-old boy

underwent a second surgical intervention at 4 years after the first operation and remained symptom- and tumor progression-free until now, 15 years following the second surgery. A 27-year-old female also with local tumor recurrence is scheduled to undergo a repeat surgery in the near future. All remaining patients repeatedly showed stable serial MRIs and remained in excellent condition after surgery.

13.5.4.3 Anaplastic Astrocytoma

Despite harboring a high-grade tumor, the vast majority of patients with anaplastic astrocytoma (11/14) also did not experience new neurological deterioration after surgery. There were only mild additional symptoms, such as sensory deficits or a deteriorating facial palsy in three other individuals. Fortunately, no surgical complications were observed in the 14 patients suffering from anaplastic astrocytoma. To prevent aspiration pneumonia due to exacerbation of pre-existing dysphagia, one male individual required tracheostomy at 8 days after surgery. While three individuals were lost to follow-up, we know from three others that they have died from their bulbar glioma between 10 months and 3 years postoperatively. Clear tumor progression was documented in 5 of 14 patients during the follow-up period. Repeat surgery might be considered in these patients.

13.5.4.4 Glioblastoma

Gratifyingly, there was also no surgical complication in any patient harboring a glioblastoma. While one female aged 24 years did not deteriorate neurologically after surgery, augmentation of pre-existing symptoms was observed in the remaining four individuals. Two of them required postoperative tracheostomy for 3 and 4 months, respectively. In all patients, the tumor eventually progressed despite combined radio-chemotherapy after surgery. One male aged 43 years with hypermethylated MGMT promoter underwent a second surgical intervention at 2 years after the initial operation and survived in an excellent clinical condition for additional 2 years until he died from diffuse local tumor recurrence. The remaining four patients died between 8 months and 2.5 years after surgery. Postoperatively, all patients did well according to the circumstances, and in all patients, surgery did favorably modify the course of the disease, at least for a certain time period. According to the preoperative clinical condition with rapid neurological deterioration, as well as taking into account the preoperative MRIs, none of the five glioblastoma patients would have survived more than a few months at most without surgical intervention.

13.6 Conclusion

From reviewing the pertinent literature, it is known that many physicians regard bulbar gliomas at first glance as inoperable lesions. However, with a reasonable patient selection policy, microsurgical tumor removal is feasible even in complex

lesions as demonstrated in this chapter, with an acceptable resection rate, good to excellent outcome, and a very low complication rate. The authors are convinced that surgery plays an important role in the overall management of medullary gliomas. In the context of modern molecular diagnosis, tumor sampling may gain even more importance in the near future. Continuous electrophysiological monitoring during surgery is helpful in guiding tumor resection and in avoiding surgical complications. A flexible attitude of the surgeon during the microsurgical intervention, for instance by not attempting an ideally high tumor resection rate in diffuse lesions that lack clear demarcation from the bulbar parenchyma, may help in avoiding irreversible damage to the medulla. On the other hand, radical tumor resection should be attempted in at least all focal low-grade tumors that are well-discernable from the brainstem parenchyma, since the tumor resection rate may favorably influence the patient's long-term outcome and survival. The final decision regarding the degree of tumor volume reduction, however, should always be taken during surgery, based on the local circumstances and specific tumor tissue properties. While a desirable resection rate, as well as a good-to-excellent outcome can be achieved also in grade III bulbar gliomas, surgery may influence the natural history of bulbar glioblastomas in a positive manner.

References

1. Babu R, Kranz PG, Agarwal V, McLendon RE, Thomas S, Friedman AH, et al. Malignant brainstem gliomas in adults: clinicopathological characteristics and prognostic factors. J Neuro-Oncol. 2014;119(1):177–85.
2. Bertalanffy H, Tsuji Y, Banan R, Kar S. Adult brainstem gliomas. In: Spetzler RF, Kalani MYS, Lawton MT, editors. Surgery of the brainstem. New York: Thieme; 2019.
3. Brat DJ, Aldape K, Colman H, Holland EC, Louis DN, Jenkins RB, et al. cIMPACT-NOW update 3: recommended diagnostic criteria for diffuse astrocytic glioma, IDH-wildtype, with molecular features of glioblastoma, WHO grade IV. Acta Neuropathol. 2018;136(5):805–10.
4. Bricolo A. Surgical management of intrinsic brain stem gliomas. Oper Tech Neurosurg. 2000;3(2):137–54.
5. Capper D, Jones DTW, Sill M, Hovestadt V, Schrimpf D. SturmD, et al. DNA methylation-based classification of central nervous system tumours. Nature. 2018;555(7697):469–74.
6. El Ahmadieh TY, Plitt A, Kafka B, Aoun SG, Raisanen JM, Orr B, et al. H3 K27M mutations in thalamic pilocytic astrocytomas with anaplasia. World Neurosurg. 2019;124:87–92.
7. Ellezam B, Theeler BJ, Walbert T, Mammoser AG, Horbinski C, Kleinschmidt-DeMasters BK, et al. Low rate of R132H IDH1 mutation in infratentorial and spinal cord grade II and III diffuse gliomas. Acta Neuropathol. 2012;124(3):449–51.
8. Gessi M, Capper D, Sahm F, Huang K, von Deimling A, Tippelt S, et al. Evidence of H3 K27M mutations in posterior fossa ependymomas. Acta Neuropathol. 2016;132(4):635–7.
9. Gupta K, Orisme W, Harreld JH, Qaddoumi I, Dalton JD, Punchihewa C, et al. Posterior fossa and spinal gangliogliomas form two distinct clinicopathologic and molecular subgroups. Acta Neuropathol Commun. 2014;2:18.
10. Hartmann C, Meyer J, Balss J, Capper D, Mueller W, Christians A, et al. Type and frequency of IDH1 and IDH2 mutations are related to astrocytic and oligodendroglial differentiation and age: a study of 1,010 diffuse gliomas. Acta Neuropathol. 2009;118(4):469–74.

11. Hu J, Western S, Kesari S. Brainstem Glioma in Adults. Front Oncol. 2016;6:180.
12. Hundsberger T, Tonder M, Hottinger A, Brugge D, Roelcke U, Putora PM, et al. Clinical management and outcome of histologically verified adult brainstem gliomas in Switzerland: a retrospective analysis of 21 patients. J Neuro-Oncol. 2014;118(2):321–8.
13. Jallo GIFD, Roonprapunt C, Epstein F. Current management of brainstem gliomas. Ann Neurosurg. 2003;3(1):1–17.
14. Javadi SA, Hartmann C, Walter GF, Banan R, Samii A. IDH1 mutation in brain stem glioma: case report and review of literature. Asian J Neurosurg. 2018;13(2):414–7.
15. Jones DT, Hutter B, Jager N, Korshunov A, Kool M, Warnatz HJ, et al. Recurrent somatic alterations of FGFR1 and NTRK2 in pilocytic astrocytoma. Nat Genet. 2013;45(8):927–32.
16. Joyon N, Tauziede-Espariat A, Alentorn A, Giry M, Castel D, Capelle L, et al. K27M mutation in H3F3A in ganglioglioma grade I with spontaneous malignant transformation extends the histopathological spectrum of the histone H3 oncogenic pathway. Neuropathol Appl Neurobiol. 2017;43(3):271–6.
17. Kleinschmidt-DeMasters BK, Donson A, Foreman NK, Dorris K. H3 K27M mutation in gangliogliomas can be associated with poor prognosis. Brain Pathol. 2017;27(6):846–50.
18. Koelsche C, Wohrer A, Jeibmann A, Schittenhelm J, Schindler G, Preusser M, et al. Mutant BRAF V600E protein in ganglioglioma is predominantly expressed by neuronal tumor cells. Acta Neuropathol. 2013;125(6):891–900.
19. Louis DN, et al. WHO classification and grading of tumours of the central nervous system. Revised 4th ed. World Health Organization classification of tumours. Lyon: IARC Press; International Agency for Research on Cancer; 2016.
20. Orillac C, Thomas C, Dastagirzada Y, Hidalgo ET, Golfinos JG, Zagzag D, et al. Pilocytic astrocytoma and glioneuronal tumor with histone H3 K27M mutation. Acta Neuropathol Commun. 2016;4(1):84.
21. Pekmezci M, Villanueva-Meyer JE, Goode B, Van Ziffle J, Onodera C, Grener JP, et al. The genetic landscape of ganglioglioma. Acta Neuropathol Commun. 2018;6(1):47.
22. Purohit B, Kamli AA, Kollias SS. Imaging of adult brainstem gliomas. Eur J Radiol. 2015;84(4):709–20.
23. Reers S, Krug D, Stummer W, Hasselblatt M. Malignant progression of a histone H3.3 K27M-mutated spinal pilocytic astrocytoma in an adult. Clin Neuropathol. 2017;36(2):83–5.
24. Reinhardt A, Stichel D, Schrimpf D, Sahm F, Korshunov A, Reuss DE, et al. Anaplastic astrocytoma with piloid features, a novel molecular class of IDH wildtype glioma with recurrent MAPK pathway, CDKN2A/B and ATRX alterations. Acta Neuropathol. 2018;136(2):273–91.
25. Reithmeier T, Kuzeawu A, Hentschel B, Loeffler M, Trippel M, Nikkhah G. Retrospective analysis of 104 histologically proven adult brainstem gliomas: clinical symptoms, therapeutic approaches and prognostic factors. BMC Cancer. 2014;14:115.
26. Reyes-Botero G, Giry M, Mokhtari K, Labussière M, Idbaih A, Delattre JY, et al. Molecular analysis of diffuse intrinsic brainstem gliomas in adults. J Neuro-Oncol. 2014;116(2):405–11.
27. Schindler G, Capper D, Meyer J, Janzarik W, Omran H, Herold-Mende C, et al. Analysis of BRAF V600E mutation in 1,320 nervous system tumors reveals high mutation frequencies in pleomorphic xanthoastrocytoma, ganglioglioma and extra-cerebellar pilocytic astrocytoma. Acta Neuropathol. 2011;121(3):397–405.
28. Schwartzentruber J, Korshunov A, Liu XY, Jones DT, Pfaff E, Jacob K, et al. Driver mutations in histone H3.3 and chromatin remodelling genes in paediatric glioblastoma. Nature. 2012;482(7384):226–31.
29. Sturm D, Witt H, Hovestadt V, Khuong-Quang DA, Jones DT, Konermann C, et al. Hotspot mutations in H3F3A and IDH1 define distinct epigenetic and biological subgroups of glioblastoma. Cancer Cell. 2012;22(4):425–37.
30. Theeler BJ, Ellezam B, Melguizo-Gavilanes I, de Groot JF, Mahajan A, Aldape KD, et al. Adult brainstem gliomas: correlation of clinical and molecular features. J Neurol Sci. 2015;353(1–2):92–7.

31. Wu G, Broniscer A, McEachron TA, Lu C, Paugh BS, Becksfort J, et al. Somatic histone H3 alterations in pediatric diffuse intrinsic pontine gliomas and non-brainstem glioblastomas. Nat Genet. 2012;44(3):251–3.
32. Wu G, Diaz AK, Paugh BS, Rankin SL, Ju B, Li Y, et al. The genomic landscape of diffuse intrinsic pontine glioma and pediatric non-brainstem high-grade glioma. Nat Genet. 2014;46(5):444–50.